Nano-TiO₂ inhibit cytotoxicity and osteogenic differentiation of CXCR4-transfected bone marrow mesenchymal stem cells

Changhai Liu, Yecheng Li, Qiang Zhou, Honglei Chen, Haojie Zhang, Zhonghua Ling and Zhanchao Wang*

Department of Orthopaedics, Chongming Hospital Affiliated to Shanghai University of Medicine and Health Sciences, Shanghai, China

Abstract: Mesenchymal stem cells (MSCs) are applied to clinical practice. Nanometer titanium dioxide (Nano-TiO₂) is a type of biological material with great biocompatibility. Herein, we aimed to explore Nano-TiO₂'s effects on differentiation of bone marrow MSCs (BMSCs) after transfection with CXCR4. After transfection of CXCR4 to BMSCs, we cultured BMSCs in medium containing 70 nm and 100 nm Nano-TiO₂. At the same time, BMSCs without CXCR4 transfection were cultured using 100nm Nano-TiO₂ medium and set as NC group. Then the cytotoxicity was detected by MTT assay, followed by ALP staining. Western blot and RT-qPCR were conducted to determine Runx2 and BGP expression. Application of TiO₂ (70 nm and 100 nm) decreased the viability of BMSCs (P < 0.05) and ALP activity, while ALP activity of 70 nm group was markedly greater than that of 100 nm group. After BMSCs were cultured for 7 d and 14 d, lower expression of Runx2 and BGP was noticed in BMSCs of 100 nm group relative to 70 nm group (P < 0.05), accompanied with lower CXCR4 mRNA expression. In conclusion, Nano-TiO₂ exhibited inhibitory effects on CXCR4-transfected BMSCs in a participle size-dependent manner. Increased size of nanoparticles was associated with decreased viability and greater cytotoxicity.

Keywords: Bone marrow mesenchymal stem cells; CXCR4; Cytotoxicity; Nanometer titanium dioxide; Osteogenic differentiation

Submitted on 06-09-2024 Revised on 05-04-2025 Accepted on 28-07-2025

INTRODUCTION

Repairing larger area of bone defects is a thorny problem. Although the problem can be solved by bone transplantation, the limited source of donor tissue and the risk of pathogen transmission have hindered the application of the approach (Xue et al., 2022, Chen et al., 2024, Wang et al., 2024). At present, stem cell therapy currently offers a promising clinical option for patients. The repair of bone defects involves numerous tissues and cells, with bone marrow mesenchymal stem cells (BMSCs) being one of the crucial players. During this process, BMSCs specifically bind to CXC chemokine receptor 4 (CXCR4). This BMSC-CXCR4 complex then migrates from peripheral or adjacent tissues to the injury site, where the cells differentiate into various lineages and contribute to bone defect repair (Wang et al., 2021). Titanium and titanium alloys, with great mechanical properties and compatibility with cells and tissues, have been highlighted for its promising potential on repair of bone defects. Nevertheless, researchers have identified limitations in the material during the third phase of clinical trials, which require further improved. Studies have confirmed that this type of material hardly integrates with bones in vivo and the capacity of integrating still fails to reach the ideal state. Therefore, it is necessary to improve the compatibility with bone tissue and accelerating

osseointegration has aroused researchers' attention (Zhu et al., 2023). A report has demonstrated that the negative effect of nanoparticles increases with the development of particle size. As a promising material for stem cell bone transplantation, nanometer titanium dioxide (Nano-TiO₂) particles interact with surrounding cells, such as osteoblasts and vascular endothelial cells. There is controversy over whether Nano-TiO₂ has toxicological effects on BMSCs transfection and inhibits osteogenic differentiation. Therefore, in this study, we explored Nano-TiO₂'s effects particles on differentiation of CXCR4-treated BMSCs, to provide a basis for its application as nano-biomaterials.

MATERIALS AND METHODS

Preparation of nanoparticles

A 99.9% pure titanium sheet (0.25 mm thick) was cut into a peptide sheet (1 cm × 1 cm) and then flatted. The peptide sheet was sonicated for 15 minutes, rinsed three times with double distilled water, and then washed with 75% alcohol and acetone, each for 15 minutes. Electrochemical anodization was performed to prepare TiO₂ nanotubes as follows: a titanium sheet on anode and a platinum sheet on cathode were mixed with a glycerol solution containing 0.27 M ammonium fluoride. The volume ratio of glycerol and distilled water was 1:1. Then the voltage of the direct current stabilized power was adjusted to 20 V and 30 V. The sheets were electrolyzed for 3 hours to produce nano-

^{*}Corresponding author: e-mail: zhibei28530@126.com

TiO₂ particles (70 nm and 100 nm). After reaction, titanium sheet was washed and dried with double distilled water.

Transmission electron microscope (TEM) detection

TEM (Japan Electronics Corporation, Japan, Model: 1230). Photo type: TEM. Shooting conditions: 80 kV. Procedure of negative staining experiment: (1) Remove 10 μL of the sample. (2) Absorb 10 μL of the sample and add it to the copper net to precipitate for 1 minute and the filter paper absorbed the float. (3) The copper grid was treated with 10 μL of uranyl acetate (or phosphotungstic acid dyeing solution) for 1 min. Excess liquid was then removed by blotting with filter paper. (4) Dry at room temperature for several minutes. (5) Imaging by electron microscopy at 80 kv. (6) Observation under TEM, image collection and analysis.

Preparation of CXCR4 transfection system

Distilled water was mixed with CXCR4 (0.4 mL), stirred for 7 hours under the conditions of N² and centrifuged at 1000 r/min for 30 minutes. The mixed solution was washed and dried at 70°C. The transfected CXCR4 solution was stored for further experiment.

Cell culture and transfection

Healthy subjects were recruited and provided informed consent. Bone marrow (5 mL) was extracted from each subject and preserved at 4 °C. The mononuclear cells were isolated within 24 hours. Briefly, the bone marrow was diluted with PBS and centrifuged at 400 × g for 20 minutes. After being cultured for 48 hours, the cells were regularly fed with fresh medium, which was replaced every 2 to 3 days. When reaching over 99%, cells were digested and passaged. The BMSCs at passage 3 were obtained (5×10⁵/mL) and transferred to three electrode cups with or without nanoparticles, which were divided into control group (without nanoparticles), 70 nm group (with 70 nm Nano-TiO₂), 100 nm group (with 100 nm Nano-TiO₂). The CXCR4 solution was respectively added to the three electrode cups. The electroporator was connected to a low-voltage DC power supply, as BMSCs were inoculated on the DNEN medium containing penicillin (100 U/mL), FBS (100 U/mL) and streptomycin (100 U/mL).

In order to induce BMSCs to further differentiate into osteoblasts and osteocytes, it is necessary to add dexamethasone, sodium glycerophosphate, ascorbic acid and other ingredients into the medium (day 0). At the same time, the third generation BMSCs (5×10⁵/mL) that were not transfected with CXCR4 were cultured in 100nm Nano-TiO2 medium and the other processes were the same as those of other groups and they were set as the NC group (Hu *et al.*, 2021). This study was approved by the ethnic committee of Chongming Hospital Affiliated to Shanghai University of Medicine and Health Sciences (approval number: SH20240608).

Cytotoxicity test

BMSCs of three groups were cultured in incubator for 24 hours. With solution removed, cells were stained and incubated for 10 minutes. After incubation, a fluorescence microscope was performed to observe and photograph the samples. The DMEM containing 10% MTT was added on day 3 and 7. They were removed onto 6-well plates and developed by dimethyl sulfoxide (500 μ L) to measure absorbance at 490 nm (Gan *et al.*, 2022).

ALP staining

After cultivation for 3, 7 and 14 days, BMSCs were washed and fixed. After fixing, cells were washed, soaked and reacted with NBT/BCIP for 20 minutes. Then the cells were washed with distilled water 5 times, each 5 minutes. Then the BMSCs were observed under an optical microscope.

Western blot analysis

On the 14th day of culture, BMSCs were washed with phosphate buffer twice. RIPA and PMSF homogenate solution was added to BMSCs and the mixture was centrifuged to collect supernatant, which was quantified. Then put the container in the boiling water bath for 15 minutes. Protein samples (50 μ g) were separated by SDS-PAGE for western blot.

Real time quantitative polymerase chain reaction (RT-qPCR)

RNA was extracted from treated HUVECs and then analyzed by UV scanning and agar Carbohydrate electrophoresis analysis. RT-qPCR was performed to detect G DNF mRNA expression.

Immunofluorescence

BMSC was fixed with 4% paraformaldehyde at room temperature and then washed 3 times with PBS. The cells were permeated with 0.3% Triton-X 100 for 30 min, washed with PBS 3 times and blocked in 10% normal goat serum for 30 min. BMSC on the surface of the nanomaterial were stained with rabbit polyclonal anti-CD29 and rabbit polyclonal anti-CD90 antibodies (Invitrogen). Cells were stained overnight with primary antibodies at 4°C and then washed three times with PBS. Use absorbent paper to absorb excess liquid and add diluted fluorescent secondary antibody (Goat anti-Rabbit Alexa 594). The cells were then rinsed with PBS and counterstained with DAPI (Beyotime Biotechnology Institute of Biotechnology Institute) for 10 minutes at room temperature (RT). After the other three were washed with PBS, the sample was fixed on a slide and viewed through an Olympus IX70 confocal microscope. All images are obtained with the same contrast and brightness parameters. The fluorescence intensity of individual cells was measured using the confocal microscope's built-in software. For each group, six cells with clear boundaries were selected.

Observation index

Absorbance value; ALP staining; Western blot of Runx2 (Runx2 is a key transcription factor that plays a crucial role in the differentiation of bone marrow MSCs into osteoblasts), BGP () protein content; mRNA expression of Runx2 and BGP.

Statistical analysis

Data were presented as mean \pm SD and analyzed by SPSS 17.0 software. Difference was determined through one-way ANOVA (LSD) with P < 0.05 considered as significant.

RESULTS

Characterization of TiO₂ nanoparticles and identification of BMSCs

TiO₂ nanoparticles were prepared by chemical precipitation method: TiO₂ and nanoparticles were dissolved in deionized water (1:2 ratio), stirred at 2000 r/min and the resulting black magnetic liquid was neutral after washing with deionized water. After high intensity ultrasonic grinding, dispersed and uniform TiO2 nanoparticles were obtained. When TiO2 nanoparticles were observed under electron microscope, the average diameter of round oxidized nanoparticles was 80 nm under the microscope (Fig. 1A). The morphology of the medium was shown in fig. 1B and fig. 1C. The surface cells of the nanomaterial were identified as BMSC by CD29 and CD90 immunofluorescence staining (Fig. 1D). After 24h of culture, SEM images of BMSC adhesion were displayed on the surface of various TiO2 nanoparticles, indicating that all BMSC were polygonal and well distributed and the attachment morphology was basically similar on the surface of the nanoparticles, but the number of attached cells was different (Fig. 2A-D). BMSC on TiO2 nanoparticles exhibit more round flakes and fewer filaments (Fig. 2C).

Cytotoxicity

With staining, under microscope, we found no difference in toxicity between the groups after 1 day of culture (Fig. 3A). Then MTT experiment indirectly reflected the cytotoxicity of BMSCs. Importantly, the results revealed that on the 7th day, optical density of control group increased most significantly, higher than 70 nm and 100 nm group (Fig. 3B).

ALP activity

After treatment with Nano-TiO₂, over time, the ALP activity of each group increased first and then decreased after day 7 (the highest value on the 7^{th} day). Nano-TiO₂ treatment effectively decreased the ALP activity of BMSCs, as demonstrated with higher value. On day 3, no difference was found between 70 nm group and 100 nm group. But after day 7, ALP activity of 70 nm group significantly outnumbered than 100 nm group (P<0.05, Fig. 4).

Expression of Runx2, BGP and CXCR4

After 7 and 14 days of culture, the expression levels of Runx2 and BGP in BMSCs of each group were significantly different (P < 0.05). The expression levels of Runx2 and BGP in the 70 nm group were significantly lower than those in the 100 nm group (P < 0.05). Compared with the control group, the expression of Runx2 and BGP decreased in both the 70 nm and 100 nm groups (P < 0.05, Fig. 5A-B).

RT-qPCR analysis showed that the mRNA expression levels of Runx2, BGP, and CXCR4 in the control group were significantly higher than those in the 70 nm and 100 nm groups on both day 7 and day 14 (P < 0.05), and the expression level in the 100 nm group was lower than that in the 70 nm group (Fig. 5C-E).

Protein expression levels of LPL, runx2 and BGP

After 7 and 14 days of culture in the osteogenic induction system, the protein expression levels of Runx2 and BGP were significantly different among the groups (P < 0.05). The Runx2 and BGP protein expression levels in both the 100 nm and 70 nm groups were lower than those in the blank control group (P < 0.05). The protein levels in the 100 nm group were significantly lower than those in the blank control group (P < 0.05). The LPL protein expression levels in MSCs of each group were significantly different (P < 0.05). The LPL expression level in the 100 nm group was higher than that in the blank control group (P < 0.05). The LPL levels in both the 100 nm and 70 nm groups were higher (P < 0.05). The results are shown in fig. 6.

DISCUSSION

BMSCs are currently one of the most commonly used cells for stem cell therapy against bone defects (Zhuang et al., 2021). These cells are characterized by a strong capacity in vitro proliferation and multi-directional differentiation potential. While the rapid development of nanotechnology brings numerous conveniences to society, it may also pose various potential risks. Nano-TiO2 has received extensive attention in recent years and its secure application becomes a spotlight. Many scholars have investigated the cytotoxicity of this material, yet its specific toxic effects remain incompletely understood. Despite this lack of comprehensive safety data, the material has been widely adopted in clinical orthopedics as a novel bone graft material. Therefore, the cytotoxicity of TiO₂ toward BMSCs and its potential inhibitory effect on osteoblast differentiation require urgent clarification (Habib *et al.*, 2023).

To further study the effect of Nano-TiO₂ size on cytotoxicity, BMSCs transfected with CXCR4 were cultured with Nano-TiO₂ (70 nm, 100 nm). Figs 3 and 4 reflected that Nano-TiO₂ had inhibitory effects on BMSCs in a size-dependent manner (Wang *et al.*, 2023, Li *et al.*, 2025).

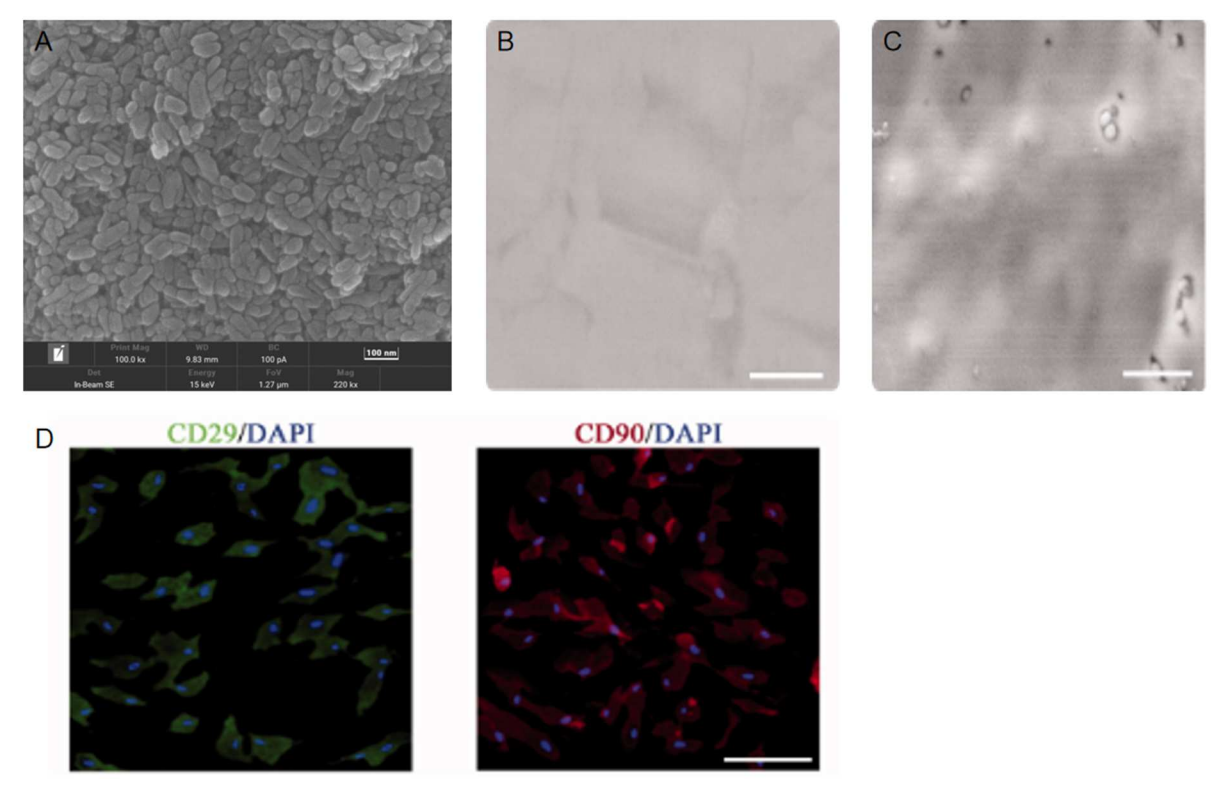


Fig. 1: Electron microscopic observation of TiO2 nanoparticles and identification of mesenchymal stem cells. (A) The morphology of TiO2 nanoparticles (100nm) was observed by SEM. (B) The morphology of CXCR4 medium (800nm) was observed by SEM. (C) The morphology of ordinary medium (800nm) was observed by SEM. (D) The surface of the nanomaterial w as determined to be BMSC (100μm) using CD29 (green) and CD90 (red).

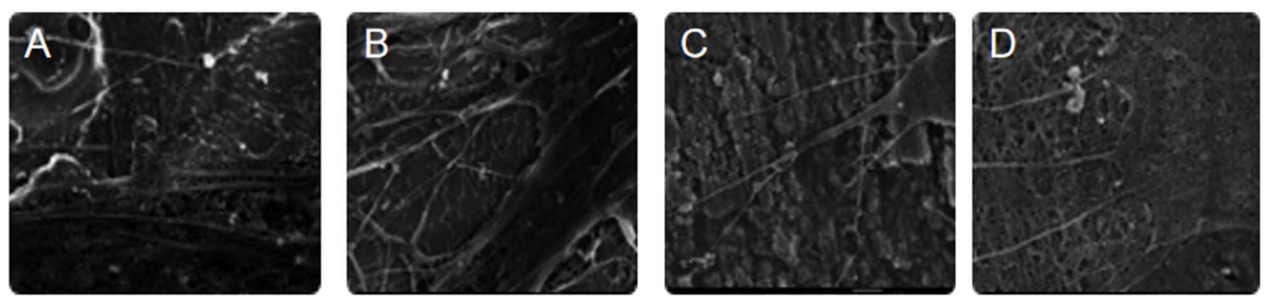


Fig. 2: The morphology of BMSC cultured on the surface of TiO2 nanoparticles was observed by SEM. (A) Untreated raw TiO2 nanoparticles. (B) TiO2 nanoparticle surface during culture. (C) The surface of TiO2 nanoparticles anodize d at 30v during culture. (D) TiO2 nanoparticles anodized at 30v for 24h. (× 50,000)

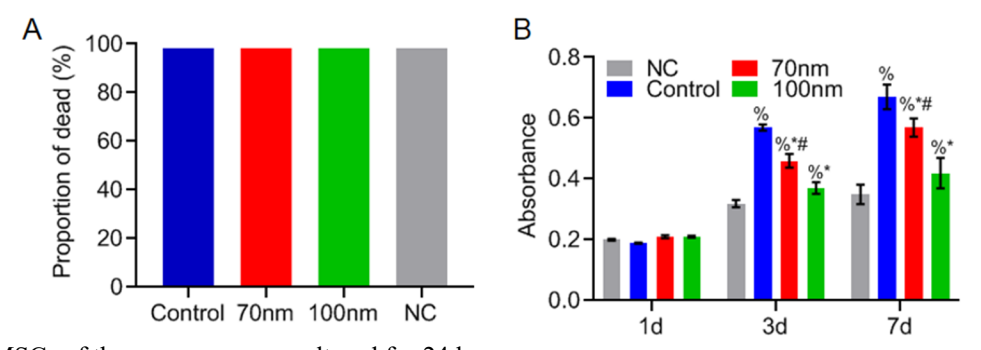


Fig. 3: (A) BMSCs of three groups were cultured for 24 hours. With solution removed, cells were stained and incubated for 10 minutes. After that, a fluorescence microscope was performed to observe the dead cells. The quantification of cell viability was performed (×200). (B) MTT assay of cytotoxicity at day 7 after treatment. % P < 0.05 vs. NC group; * P < 0.05 vs. Control group; # P < 0.05 vs. 100 nm group.

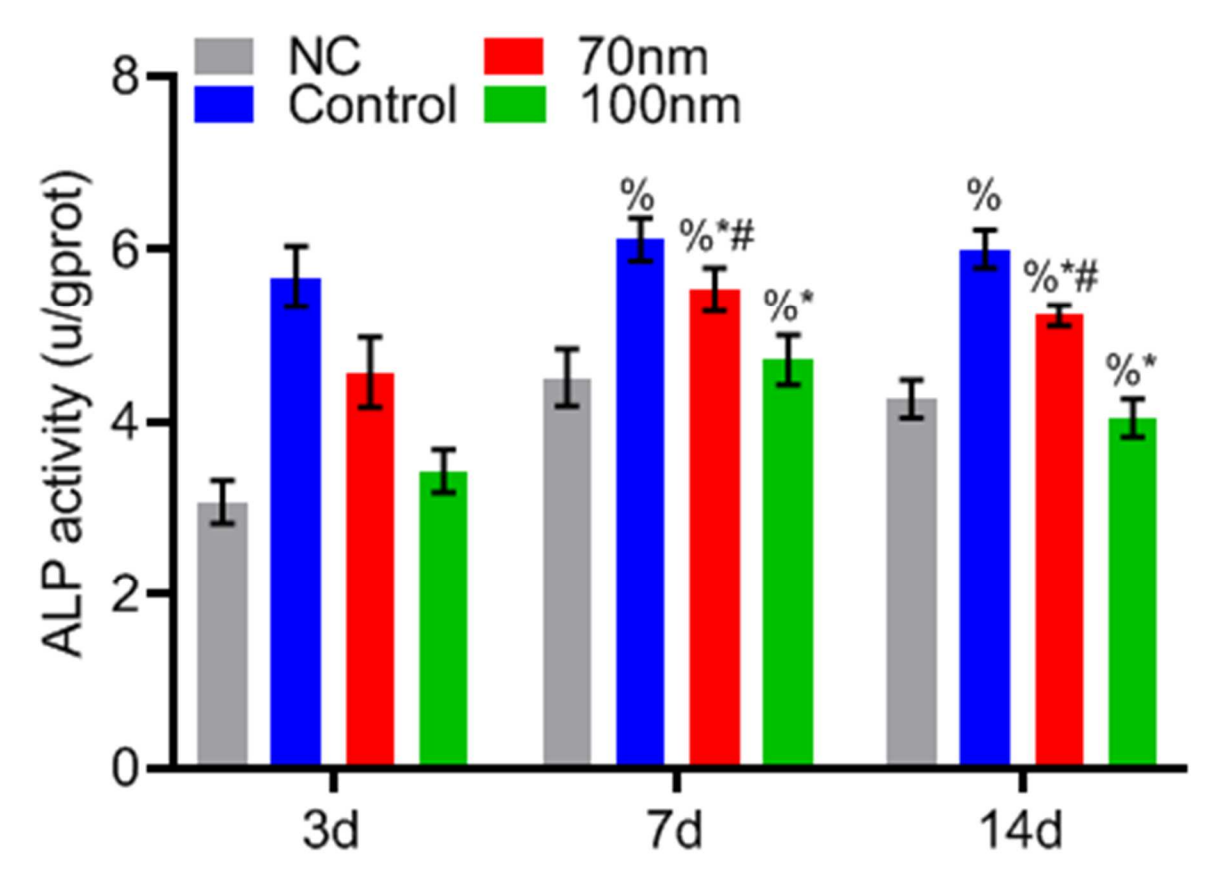


Fig. 4: ALP activity on day 3, 7 and 14 after osteogenic induction. % P < 0.05 vs. NC group; * P < 0.05 vs. Control group; # P < 0.05 vs. 100 nm group.

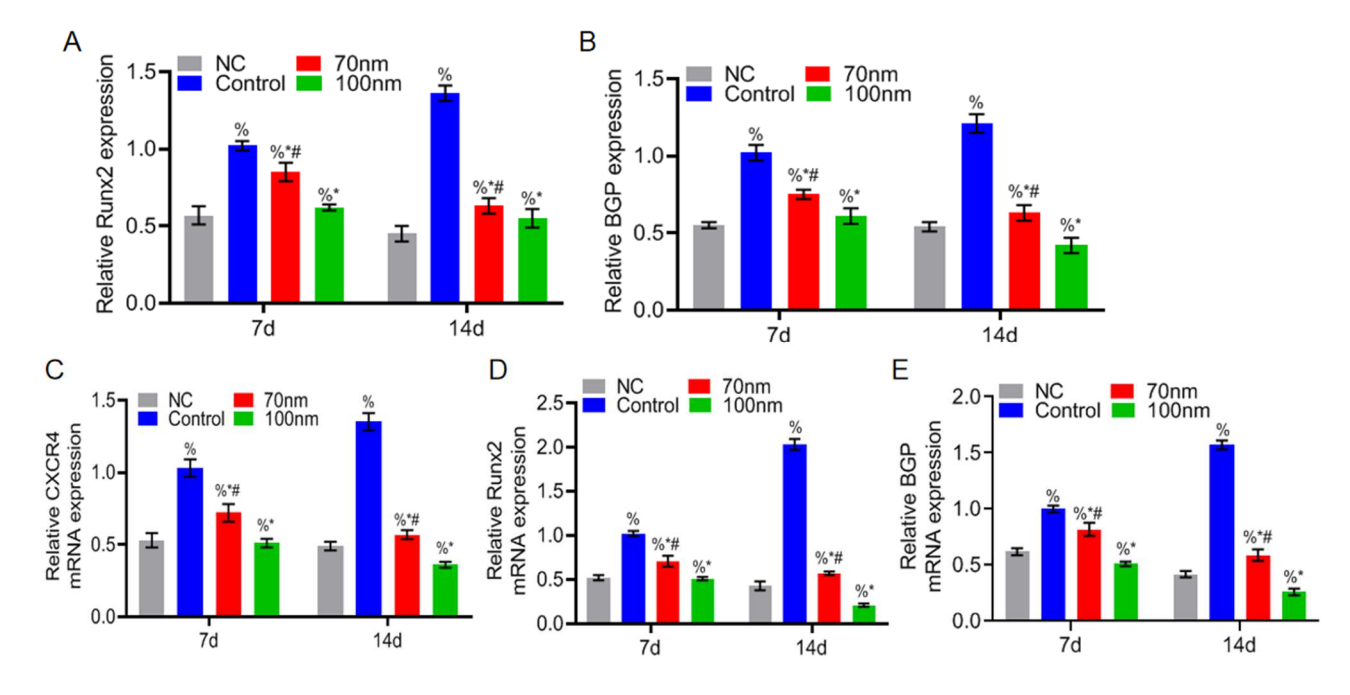


Fig. 5: The expression of Runx2, BGP and CXCR4. (A) Runx2 protein expression in each group. (B) BGP protein expression upon treatment with Nano-TiO₂ or Controls. (C) RT-qPCR analysis of CXCR4 mRNA expression. (D) Runx2 mRNA content of groups. (E) RT-qPCR of BGP mRNA content. % $P < 0.05 \ vs$. NC group; * $P < 0.05 \ vs$. Control group; # $P < 0.05 \ vs$. 100 nm group.

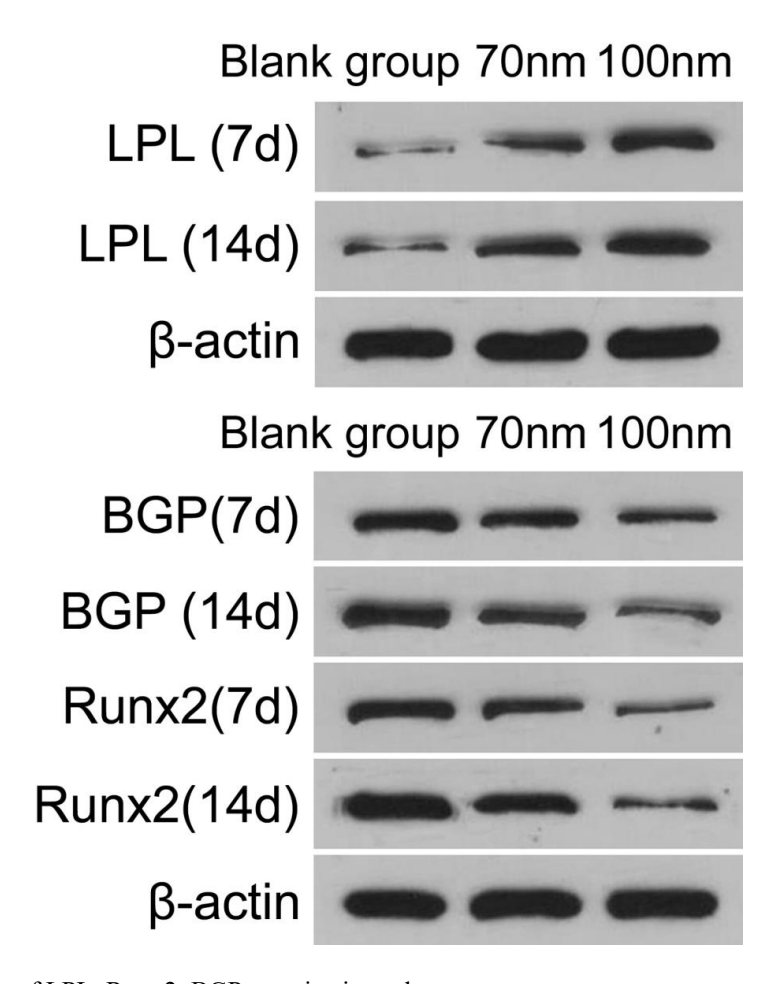


Fig. 6: Expression levels of LPL, Runx2, BGP proteins in each group.

Moreover, we found that the larger nanoparticles exhibited greater inhibitory effect on proliferation. Mechanisms (Gu et al., 2025, Zhang et al., 2025, Ye et al., 2021, Sun et al., 2021) might be the reasons: 100 nm nanoparticles change the acidity in the cell, thereby inhibiting cell viability and proliferation.

ALP is a glycoprotein involved in the process of calcium binding and transport (Le-Vinh et al., 2022, Virdi et al., 2022). It can inactivate calcification inhibitor and accelerate the calcification of bone cells. This process enables the calcium and phosphorus on the amino acid residues to combine, thereby stimulating bone calcification. Therefore, ALP is one of the enzymes that functions in osteoblasts (Nian et al., 2022, Zhang et al., 2025, Ye et al., 2021, Greither et al., 2020, Sun et al., 2021, Zhang et al., 2022) and serves as an indicator of early differentiation activity when inducing osteogenic differentiation of BMSCs (Ma et al., 2023, Wu et al., 2023). In this experiment, the results of ALP staining during the osteogenic differentiation of BMSCs showed that BMSCs treated with Nano-TiO₂ (70 nm group and 100 nm group) exhibited osteogenic differentiation inhibition in the early stage of osteogenic differentiation. It may be because Nano-TiO₂ inhibits the protein synthesis of osteogenic differentiation and prevents BMSCs from differentiating into osteogenic cells.

The mineralization period is the final stage of BMSCs osteogenic differentiation, characterized by the formation of hydroxyapatite crystals that are visible under microscopy. In contrast, Bone Gla Protein (BGP) is secreted abundantly during the late stage of bone differentiation. It inhibits hydroxyapatite crystal formation, prevents bone nodule formation, and yet still contributes to the overall bone formation process. Therefore, BGP can be used as an accurate indicator to reflect the activity of bone cells formed after differentiation (Ma et al., 2023, Hatt et al., 2023, Greither et al., 2020). In this work, Runx2 and BGP expression was measured in BMSCs of each group. Osteogenic differentiation of BMSCs in the 70 nm and 100 nm groups was low. It is probably that Nano-TiO₂ up-regulates the expression of mRNA on the BMSCs transfected with CXCR4 (Greither et al., 2020, Wang et al., 2023, Kang et al., 2023) and down-regulates the secretion of proteins related to osteogenic differentiation such as ALP, BGP and Runx2. It can effectively inhibit the osteogenic differentiation of BMSCs (Hu et al., 2021, Khrunyk et al., 2020).

As we all know, cell adhesion, growth and differentiation are important parameters to evaluate the biocompatibility of nanomaterials and the effects of the structure of nanomaterials on cells are also different (Oin et al., 2022). In the results of this study, it can be found that during BMSC cell culture and 24h after culture, the cell front of TiO2 nanoparticles showed irregular filamentin and it has been confirmed in previous studies that there is a close relationship between the morphology and differentiation of these cells and they can induce bone formation by reducing the diffusion area of cells (Donsante et al., 2021, Liu et al., 2025). This suggests that the interaction between cells and nanostructures can enhance differentiation and promote the rate of osteogenic differentiation. In addition, it can also be found in this result that the structure and elements on the surface of nanomaterials can affect the adhesion effect of cells, but not their proliferation, which is also similar to the research conclusion of Kladko et al. (Kladko et al., 2021).

However, we only notice the relationship between cytotoxicity and osteogenic differentiation of BMSCs between nanomaterials of different sizes, but did not further verify the conclusion through *in vitro* and *in vivo* experiments. Cell migration experiments will be conducted in the future. Researchers have been working hard to explore relationship between levels of BMSC genes and related proteins and those factors. Many mechanisms are still not very clear, including how BMSC genes regulate stem cell migration, how the related pathways work and how to improve the therapeutic effect after transplantation of nanoscale encapsulated stem cells.

CONCLUSION

In conclusion, Nano-TiO₂ of different sizes has inhibitory effects on BMSCs transfected with CXCR4 in a size-dependent manner, indicating that it might be used as novel approach to regulate BMSCs differentiation. This study also has certain shortcomings. The relevant signal pathways involved in the regulation process was not studied. In addition, this study only focused on *in vitro* experiments but did not perform clinical research analysis or in animal models. Therefore, in the future studies, large clinical sample analysis and animal models should be used to comprehensively analyze the effect of Nano-TiO₂ on BMSCs differentiation.

Acknowledgment

Not applicable.

Authors' contributions

Changhai Liu and Zhanchao Wang: Conceptualization, Methodology, Supervision, Project administration, Funding acquisition, Writing – Review & Editing. Yecheng Li: Investigation, Data Curation, Formal analysis, Validation, Visualization, Writing – Original Draft.

Qiang Zhou and Honglei Chen: Investigation, Resources, Data Curation.

Haojie Zhang and Zhonghua Lin: Software, Validation, Formal Analysis.

All authors have read and approved the final version of the manuscript.

Funding

There was no funding.

Data availability statement

All data analyzed in this study are included in this article and its supplementary materials.

Ethical approval

This study utilized only commercially available cell lines and did not involve any experiments on humans or animals

Conflict of interest

None.

REFERENCES

- Chen Y, Gan W, Cheng Z, Zhang A, Shi P and Zhang Y (2024). Plant molecules reinforce bone repair: Novel insights into phenol-modified bone tissue engineering scaffolds for the treatment of bone defects. *Mater. Today. Bio.*, **24**: 100920.
- Donsante S, Palmisano B, Serafini M, Robey PG, Corsi A and Riminucci M (2021). From stem cells to bone-forming cells. *Int. J. Mol. Sci.*, **22**(8):3989.
- Gan L, Leng Y, Min J, Luo XM, Wang F and Zhao J (2022). Kaempferol promotes the osteogenesis in rBMSCs via mediation of SOX2/miR-124-3p/PI3K/Akt/mTOR axis. *Eur. J. Pharmacol.*, **927**: 174954.
- Greither T, Wenzel C, Jansen J, Kraus M, Wabitsch M and Behre HM (2020). MiR-130a in the adipogenesis of human SGBS preadipocytes and its susceptibility to androgen regulation. *Adipocyte.*, **9**(1): 197-205.
- Gu WJ, Zhao FZ, Huang W, Zhu MG, Huang HY, Yin HY and Chen T (2025). Selenium nanoparticles activate selenoproteins to mitigate septic lung injury through miR-20b-mediated RORγt/STAT3/Th17 axis inhibition and enhanced mitochondrial transfer in BMSCs. *J Nanobiotechnology.*, **23**(1): 226.
- Habib S, Rashid F, Tahir H, Liaqat I, Latif AA, Naseem S, Khalid A, Haider N, Hani U, Dawoud RA, Modafer Y, Bibi A and Jefri OA (2023). Antibacterial and cytotoxic effects of biosynthesized zinc oxide and titanium dioxide nanoparticles. *Microorganisms*., 11(6): 1363.
- Hatt LP, van der Heide D, Armiento AR and Stoddart MJ (2023). β-TCP from 3D-printed composite scaffolds acts as an effective phosphate source during osteogenic differentiation of human mesenchymal stromal cells. *Front. Cell. Dev. Biol.*, **11**: 1258161.
- Hu H, Chen L, Li ST, Pan QY and Liu YP (2021). Nano-TiO2 particles inhibit the biological behavior and

- mineralization of bone marrow mesenchymal stem cells transfected with CXCR4. *Eur. Rev. Med. Pharmacol. Sci.*, **25**(1): 71-77.
- Kang H, Dong Y, Liu H, Luo C, Song H, Zhu M, Guo Q, Peng R, Li F and Li Y (2022). Titania-nanotube-coated titanium substrates promote osteogenesis and suppress osteoclastogenesis via integrin ανβ3. *ACS. Appl. Bio. Mater.*, **5**(12): 5832-5843.
- Khrunyk YY, Belikov SV, Tsurkan MV, Vyalykh IV, Markaryan AY, Karabanalov MS, Popov AA and Wysokowski M (2020). Surface-dependent osteoblasts response to TiO(2) nanotubes of different crystallinity. *Nanomaterials (Basel).*, **10**(2): 320.
- Kladko DV, Falchevskaya AS, Serov NS and Prilepskii AY (2021). Nanomaterial shape influence on cell behavior. *Int. J. Mol. Sci.*, **22**(10): 5266.
- Le-Vinh B, Akkus-Dagdeviren ZB, Le NMN, Nazir I and Bernkop-Schnürch A (2022). Alkaline Phosphatase: A reliable endogenous partner for drug delivery and diagnostics. *Advanced. Therapeutics.*, **5**(2): 2100219.
- Li G, Zhang Y, Wang H, Zhao Y, Liu K, Li Z, Meng M, He Y and Song W (2025). The bone marrow mesenchymal stem cells derived migrasomes induced by titania nanotubes surface serve as chemotaxis effect for osteogenesis. *J. Nanobiotechnology.*, **23**(1): 592.
- Liu L, Chen H, Zhao X, Han Q, Xu Y, Liu Y, Zhang A, Li Y, Zhang W, Chen B and Wang J (2025). Advances in the application and research of biomaterials in promoting bone repair and regeneration through immune modulation. *Mater. Today. Bio.*, **30**: 101410.
- Ma S, Li S, Zhang Y, Nie J, Cao J, Li A, Li Y and Pei D (2023). BMSC-derived exosomal CircHIPK3 promotes osteogenic differentiation of MC3T3-E1 Cells via Mitophagy. *Int. J. Mol. Sci.*, **24**(3): 2785.
- Nian F, Qian Y, Xu F, Yang M, Wang H and Zhang Z (2022). LDHA promotes osteoblast differentiation through histone lactylation. *Biochem. Biophys. Res. Commun.*, **615**: 31 35.
- Qin X, Wu Y, Liu S, Yang L, Yuan H, Cai S, Flesch J, Li Z, Tang Y, Li X, Zhuang Y, You C, Liu C and Yu C (2022). Surface modification of polycaprolactone scaffold with improved biocompatibility and controlled growth factor release for enhanced stem cell differentiation. *Front. Bioeng. Biotechnol.*, **9**: 802311.
- Sun H, Zheng K, Zhou T and Boccaccini AR (2021). Incorporation of Zinc into Binary SiO2-CaO Mesoporous bioactive glass nanoparticles enhances anti-inflammatory and osteogenic activities. *Pharmaceutics.*, **13**(12): 2124.
- Virdi GS, Choi ML, Evans JR, Yao Z, Athauda D, Strohbuecker S, Nirujogi RS, Wernick A, Pelegrina-Hidalgo N, Leighton C, Saleeb RS, Kopach O, Alrashidi H, Melandri D, Perez-Lloret J, Angelova PR, Sylantyev S, Eaton S, Heales S, Rusakov DA, Alessi DR, Kunath

- T, Horrocks MH, Abramov AY, Patani R and Gandhi S (2022). Protein aggregation and calcium dysregulation are hallmarks of familial Parkinson's disease in midbrain dopaminergic neurons. *NPJ. Parkinsons. Disease.*, **8**(1): 162.
- Wang C, Liu Y, Hu X, Shang X, Ma S, Guo H, Ma X, Cai D, Hu Z, Zhao Y, Zhu Y, Cao Z, Yu H and Cheng W (2023). Titanium dioxide nanotubes increase purinergic receptor P2Y6 expression and activate its downstream PKCα-ERK1/2 pathway in bone marrow mesenchymal stem cells under osteogenic induction. *Acta. Biomater.*, **157**: 670-682.
- Wang S, Gao S, Li Y, Qian X, Luan J and Lv X (2021). Emerging importance of chemokine receptor CXCR4 and its ligand in liver disease. *Front. Cell. Dev. Biol.*, 9: 716842
- Wang X, Xiang C, Huang C, Cheng H, Zhou Z, Zhang J and Xie H (2024). The treatment efficacy of bone tissue engineering strategy for repairing segmental bone defects under diabetic condition. *Front. Bioeng. Biotechnol.*, **12**: 1379679.
- Wu Z, Zhu J, Wen Y, Lei P, Xie J, Shi H, Wu R, Lou X and Hu Y (2023). Hmgal-overexpressing lentivirus protects against osteoporosis by activating the Wnt/β-catenin pathway in the osteogenic differentiation of BMSCs. *FASEB*. J., **37**(9): e22987.
- Xue N, Ding X, Huang R, Jiang R, Huang H, Pan X, Min W, Chen J, Duan JA, Liu P and Wang Y (2022). Bone tissue engineering in the treatment of bone defects. *Pharmaceuticals (Basel).*, **15**(7): 879.
- Ye Y, Liu Q, Li C and He P (2021). miR-125a-5p regulates osteogenic differentiation of human adipose-derived mesenchymal stem cells under oxidative stress. *Biomed. Res. Int.*, **2021**: 6684709.
- Zhang S, Xie Y, Yan F, Zhang Y, Yang Z, Chen Z, Zhao Y, Huang Z, Cai L and Deng Z (2022). Negative pressure wound therapy improves bone regeneration by promoting osteogenic differentiation via the AMPK-ULK1-autophagy axis. *Autophagy*., **18**(9): 2229-2245.
- Zhang W, Zhang Y, Hao Z, Yao P, Bai J, Chen H, Wu X, Zhong Y and Xue D (2025). Synthetic nanoparticles functionalized with cell membrane-mimicking, bonetargeting, and ROS-controlled release agents for osteoporosis treatment. Journal of controlled release: official *J. Control. Release.*, **378**: 306-319.
- Zhu W, Li C, Yao M, Wang X, Wang J, Zhang W, Chen W and Lv H (2023). Advances in osseointegration of biomimetic mineralized collagen and inorganic metal elements of natural bone for bone repair. *Regen. Biomater*, **10**: 030.
- Zhuang WZ, Lin YH, Su LJ, Wu MS, Jeng HY, Chang HC, Huang YH and Ling TY (2021). Mesenchymal stem/stromal cell-based therapy: Mechanism, systemic safety and biodistribution for precision clinical applications. *J. Biomed. Sci.*, **28**(1): 28.